Electronic Research Archive

http://www.aimspress.com/journal/era

ERA, 31(11): 6964–6981.
DOI: 10.3934/era.2023353
Received: 14 June 2023
Revised: 11 October 2023
Accepted: 24 October 2023
Published: 30 October 2023

Research article

Amplitude death, oscillation death, and stable coexistence in a pair of VDP oscillators with direct–indirect coupling

Xiaojun Huang[1,2], **Zigen Song**[1,*] **and Jian Xu**[1]

[1] School of Aerospace Engineering and Applied Mechanics, Tongji University, Shanghai 200092, China

[2] Institute of Theoretical Physics, Shanxi University, Taiyuan 030006, China

* **Correspondence:** Email: zgsong@tongji.edu.cn.

Abstract: In this paper, we investigated the dynamics of a pair of VDP (Van der Pol) oscillators with direct-indirect coupling, which is described by five first-order differential equations. The system presented three types of equilibria including HSS (homogeneous steady state), IHSS (inhomogeneous steady state) and NPSS (no-pattern steady state). Employing the corresponding characteristic equations of the linearized system, we obtained the necessary conditions for the pitchfork and Hopf bifurcations of the equilibria. Further, we illustrated one-dimensional bifurcation and phase diagrams to verify theoretical results. The results show that the system exhibited two types of oscillation quenching, i.e., amplitude death (AD) for HSS equilibria and oscillation death (OD) for IHSS equilibria. In some special regions of the parameters, the system proposed multiple types of stable coexistence including HSS and IHSS equilibria, periodic orbits or quasi-periodic oscillations.

Keywords: VDP oscillator; direct-indirect coupling; oscillation death; bifurcation; multistability

1. Introduction

Pattern formation and cooperative behaviors of oscillator units linked through different interactions have become an interesting and important researching topic in a broad range of natural systems. Many phenomena, such as synchronization, phase locking, amplitude death (AD) and oscillation death (OD), can be observed in interaction systems between the coupled nonlinear oscillators [1–3].

Depending on stability analysis of an equilibrium state, the system presents stable stationary and oscillatory with homogeneous or inhomogeneous patterns. There are two types of oscillation quenching, AD and OD. To be specific, AD corresponds to the homogeneous steady state (HSS) [4], which has potential application in many couplied systems such as lasers [5], oceanography [6], multi-module floating airports [7], electronic circuits [8, 9] and neuronal systems [10]. By contrast, OD means in-

homogeneous steady states (IHSS) [11], which has implications in comprehending biological systems, including neural networks [12], genetic oscillations [13] and cell differentiation [14]. When natural frequencies of two lasers are close, the injection of light from an uncontrolled diode laser into an outer cavity has been discovered to result in the halting of oscillation – a phenomenon referred to as the OD [5]. Further, the coupling model of the common atmosphere between the North Pacific and North Atlantic can cause decadal variability of two oceans to reach an OD state [6]. In the dual-cell inhibitory neural network, researchers have also observed that when coupling intensity is weakened, the periodic activity between two neuronal populations disappears; that is, the OD state appears [12]. In electronic circuits, researchers often use circuit components to construct circuit systems to verify various homogeneous or inhomogeneous behaviors, including AD and OD states [15].

In this study, the Van der Pol (VDP) oscillators with a direct–indirect coupling scheme will be presented to reveal complex dynamical behaviors, including oscillation quenching with OD and AD, periodic oscillation, quasi-periodic orbits and their coexistence. As a matter of fact, there is a long history of researches on the VDP oscillator, which is a classical model of the self-oscillating system described by a second-order ordinary differential equation (ODE). A thorough summary for the VDP oscillator has been conducted in the themonograph by Nayfeh and Mook [16]. The VDP oscillator model can be implemented in electronic circuits [15], cryptography [17], aeroelasticity [18] and even quantum mechanics [19]. For the coupling VDP oscillators, some types of coupling schemes have been applied, which includes weakly coupling with time delay [20], indirect coupling [21], and dynamical coupling [22]. Further, modal analysis of the coupled system with a large number of VDP oscillators was carried to obtain the existence of nondegenerate and degenerate modes [23]. However, there are few researching results on the VDP coupled system with direct–indirect coupling. The corresponding mathematical model was proposed by Resmi et al. [24], which is

$$\begin{cases} dx_{11}/dt = x_{12} + d(x_{21} - x_{11}) + ey, \\ dx_{12}/dt = a(1 - x_{11}^2)x_{12} - x_{11}, \\ dx_{21}/dt = x_{22} + d(x_{11} - x_{21}) + ey, \\ dx_{22}/dt = a(1 - x_{21}^2)x_{22} - x_{21}, \\ dy/dt = -ky - e(x_{11} + x_{21})/2, \end{cases} \tag{1.1}$$

where x_{i1}, x_{i2} are activities of the i-th oscillator, a is the nonlinear damping ratio, d is the coupling strength of the direct coupling, the state variable y denotes the indirect coupling of the external environment, which is modeled by a one-dimensional over-damped oscillator with damping parameter k and the parameter e is a coupling strength between systems and environment. Resmi et al. [24] provided a general stability analysis to obtain the general mechanism of the AD for the direct–indirect coupling system. They found that the dynamical transitions of the AD fall into two types, continuous and discontinuous. Ghosh and Banerjee [9] presented a detailed bifurcation analysis and found the OD and a novel nontrvial AD (NAD) state, which is a nonzero bistable HSS. In this study, we present a more comprehensive analysis of the direct–indirect coupling VDP system and find more oscillation quenching states, one trivial equilibrium and three types of coupling-dependent nontrivial equilibria, i.e., IHSS, HSS, and no-pattern steady state (NPSS). In fact, the NPSS represents a steady state with neither a symmetrical nor anti-symmetrical steady state. It was also observed in the Lorenz system with direct-indirect coupling [25], and it may have many applications in many real systems, such as laser [26] and geomagnetic [27]. Besides, based on the theoretical analysis and numerical simulations,

we further propose multiple types of stable coexistence including the coexistence of two oscillations, the coexistence of oscillations and equilibria and the coexistence of multiple equilibria.

This paper is organized as follows. In section one, we propose the VDP oscillator model with direct-indirect coupling. In section two, the stability of the equilibria and their corresponding bifurcations including pitchfork and Hopf bifurcations are presented by theoretical analysis. The system presents three types of equilibrium, HSS, IHSS and NPSS, in the different regions of the parameters. In section three, we present numerical analysis in a wide range of parameter regions and illustrate a two-parameter bifurcation diagram by using the differential equations tool named XPPAUT [28], which can be easily used for time series analysis, phase space analysis, variable parameter analysis and bifurcation analysis, etc. The corresponding one-dimensional bifurcations and time histories for the fixed parameters are then illustrated to explicate and validate theoretical analyses, and the VDP oscillator with direct-indirect coupling illustrates multiple complex dynamical behaviors including AD and OD, periodic and quasi-periodic oscillations, and their stability coexistence. Conclusions and discussions are given in section four.

2. Stability analysis of the equilibrium

We first perform the equilibrium and its stability of system (1.1). It follows that the coupling VDP oscillator has one trivial equilibrium $O(0,0,0,0,0)$ and three types of coupling-dependent nontrivial equilibria:

(i) IHSS $A^{\pm}(\pm x_{11}^{A}, \pm x_{12}^{A}, \mp x_{11}^{A}, \mp x_{12}^{A}, 0)$, is expressed as $x_{11}^{A} = \sqrt{2ad-1}/\sqrt{2ad}$ and $x_{12}^{A} = \sqrt{2d(2ad-1)}/\sqrt{a}$.

(ii) HSS $B^{\pm}(\pm x_{11}^{B}, \pm x_{12}^{B}, \pm x_{11}^{B}, \pm x_{12}^{B}, \mp y^{B})$, is expressed as $x_{11}^{B} = \sqrt{ae^2-k}/(e\sqrt{a})$,$x_{12}^{B} = e\sqrt{ae^2-k}/(k\sqrt{a})$, and $y^{B} = \sqrt{ae^2-k}/(k\sqrt{a})$.

(iii) NPSS $C^{\pm}(\pm x_{11}^{C}, \pm x_{12}^{C}, \mp x_{21}^{C}, \mp x_{22}^{C}, \pm y^{C})$, $D^{\pm}$ $(\pm x_{11}^{D}, \pm x_{12}^{D}, \mp x_{21}^{D}, \mp x_{22}^{D}, \pm y^{D})$ are expressed as

$$x_{11}^{C} = \frac{(\Delta_1 + \sqrt{\Delta_2})}{a(e^4 - 4d^2k^2)}\sqrt{\frac{\Delta_1 - \sqrt{\Delta_2}}{a(e^2+2dk)^2}}, x_{21}^{C} = \sqrt{\frac{\Delta_1 - \sqrt{\Delta_2}}{a(e^2+2dk)^2}},$$
$$x_{11}^{D} = \frac{(\Delta_1 - \sqrt{\Delta_2})}{a(e^4 - 4d^2k^2)}\sqrt{\frac{\Delta_1 + \sqrt{\Delta_2}}{a(e^2+2dk^2)}}, x_{21}^{D} = \sqrt{\frac{\Delta_1 + \sqrt{\Delta_2}}{a(e^2+2dk)^2}},$$

where $\Delta_1 = ae^4 - e^2k + 2d(2ad-1)k^2$, $\Delta_2 = k(e^2+2dk(1-4ad))(k(e^2+2dk)-2ae^4)$, and x_{12}^{C}, x_{12}^{D},x_{22}^{C},x_{22}^{D}, y^{C}, y^{D} are subjected to

$$x_{12}^{C(D)} = \frac{x_{11}^{C(D)}}{a(1 - x_{11}^{C(D)^2})}, x_{22}^{C(D)} = \frac{x_{21}^{C(D)}}{a(1 - x_{21}^{C(D)^2})}, y^{*} = \frac{e(x_{11}^{C(D)} + x_{21}^{C(D)})}{2k}.$$

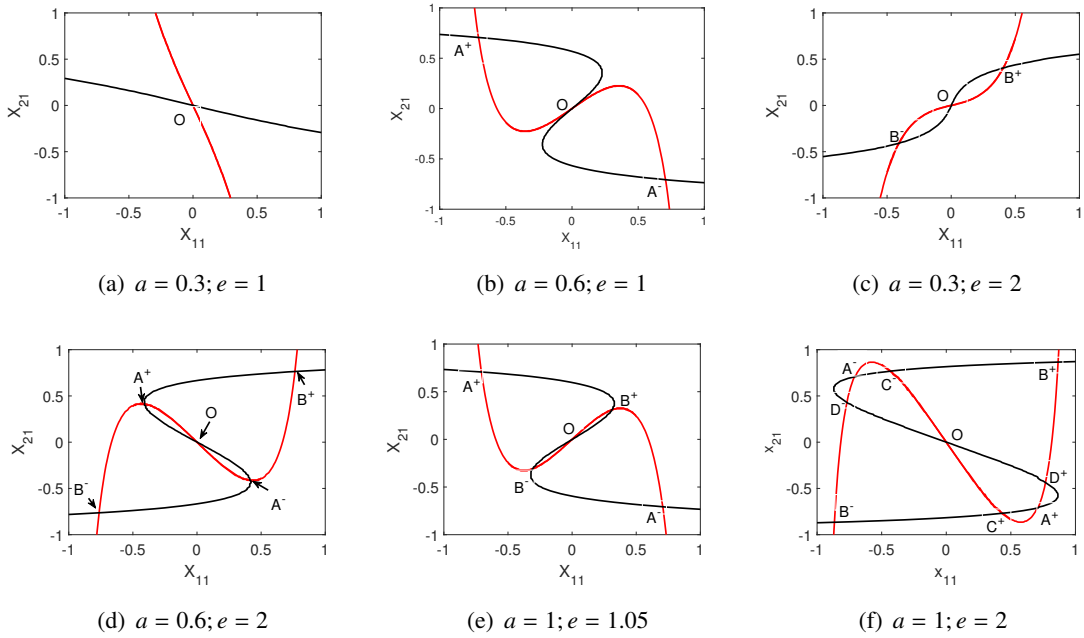

(a) $a = 0.3; e = 1$ (b) $a = 0.6; e = 1$ (c) $a = 0.3; e = 2$

(d) $a = 0.6; e = 2$ (e) $a = 1; e = 1.05$ (f) $a = 1; e = 2$

Figure 1. The intersection points of the system's nullclines show a number of equilbria with the fixed parameters $d = 1, k = 1$, where O is the trivial equilibrium, $A^{\pm}$ means the IHSS equilibrium, $B^{\pm}$ means the HSS equilibrium and $C^{\pm}$ and $D^{\pm}$ are the NPSS equilibria.

In order to illustrate the equilibria of system (1.1), we choose a-e as adjustable parameters for the fixed $d = 1$ and $k = 1$. The nullcline diagrams are exhibited in Figure 1. It follows that the system has only one trivial equilibrium O for $a = 0.3$ and $e = 1$, as shown in Figure 1(a). When $a = 0.6$ and $e = 1$, the system presents three equilibria, which is the trivial equilibrium O and a pair of IHSS equilibrium $A^{\pm}$, as shown in Figure 1(b). Conversely, if $a = 0.3$ and $e = 2$, the system has the trivial equilibrium O and a pair of HSS equilibrium $B^{\pm}$, as shown in Figure 1(c). When $a = 1$, $e = 1.05$ and $a = 0.6$, $e = 2$ and the system will propose the trivial equilibrium O, a pair of IHSS equilibrium $A^{\pm}$ and a pair of HSS equilibrium $B^{\pm}$, as shown in Figure 1(d),(e), respectively. Further, when $a = 1$, $e = 2$, the system illustrates nine equilibria, which is the trivial equilibrium O, a pair of IHSS equilibrium $A^{\pm}$, a pair of HSS equilibrium $B^{\pm}$, and two pairs of NPSS equilibria $C^{\pm}$, $D^{\pm}$, as shown in Figure 1(f).

We rewrite these equilibria as $(\bar{x}_{11}, \bar{x}_{12}, \bar{x}_{21}, \bar{x}_{22}, \bar{y})$ for analyzing its stability and their bifurcations including pitchfork and Hopf bifurcations. The Jacobian matrix of system (1.1) at the equilibria $(\bar{x}_{11}, \bar{x}_{12}, \bar{x}_{21}, \bar{x}_{22}, \bar{y})$ is obtained as

$$J = \begin{pmatrix} -d & 1 & d & 0 & e \\ -1 - 2a\bar{x}_{11}\bar{x}_{12} & a(1-\bar{x}_{11}^2) & 0 & 0 & 0 \\ d & 0 & -d & 1 & e \\ 0 & 0 & -1 - 2a\bar{x}_{21}\bar{x}_{22} & a(1-\bar{x}_{21}^2) & 0 \\ -e/2 & 0 & -e/2 & 0 & -k \end{pmatrix}. \tag{2.1}$$

The characteristic equation for the trivial equilibrium $O(0, 0, 0, 0, 0)$ is expressed as follows

$$(\lambda^2 + (2d - a)\lambda - 2ad + 1)(\lambda^3 + (k - a)\lambda^2 + (e^2 - ak + 1)\lambda - ae^2 + k) = 0. \tag{2.2}$$

Based on the characteristic equation (2.2), we analyze the stability of the trivial equilibrium by using the Routh-Hurwitz criterion [29]. Further, system (1.1) produces a pair of nontrivial equilibrium by a pitchfork bifurcation of the trivial equilibrium. The necessary conditions for the pitchfork bifurcation, labeled as PB_1 and PB_2, can be obtained

$$PB_1 : 1 - 2ad = 0, PB_2 : k - ae^2 = 0. \tag{2.3}$$

Moreover, the periodic oscillation surrounding the trivial equilibrium can be obtained by the Hopf bifurcation. The necessary conditions for the Hopf bifurcation, i.e., HB_1 and HB_2, can be obtained

$$HB_1 : 2d - a = 0, HB_2 : (e^2 - ak + 1)(k - a) - k + ae^2 = 0. \tag{2.4}$$

Similarly, for the nontrivial IHSS equilibria $A^{\pm}$, we can obtain the corresponding characteristic equation

$$\begin{aligned}(2d\lambda^3 + (2dk - 1)\lambda^2 + (8ad^2 + 2de^2 - 2d - k)\lambda + 8ad^2k - 2dk - e^2)\\ (2d\lambda^2 + (4d^2 - 1)\lambda + 8ad^2 - 4d) = 0.\end{aligned} \tag{2.5}$$

The necessary conditions of the pitchfork bifurcation for the IHSS equilibria $A^{\pm}$, i.e., PB_3, can be obtained

$$PB_3 : 8ad^2k - 2dk - e^2 = 0. \tag{2.6}$$

The necessary conditions for the Hopf bifurcation points, i.e. HB_3 and HB_4, can be obtained

$$HB_3 : 4d^2 - 1 = 0, HB_4 : 2d(8ad^2k - 2dk - e^2) - (2dk - 1)(8ad^2 + 2de^2 - 2d - k) = 0. \tag{2.7}$$

Additional, the corresponding characteristic equation for the nontrivial HSS equilibria $B^{\pm}$ is

$$\begin{aligned}(e^2k\lambda^3 + (e^2k^2 - k^2)\lambda^2 + (2ae^4 + e^4k - e^2k - k^3)\lambda + 2ae^4k - 2e^2k^2)\\ (e^2k\lambda^2 + (2de^2k - k^2)\lambda + 2ae^4 - e^2k - 2dk^2) = 0.\end{aligned} \tag{2.8}$$

The necessary conditions of the pitchfork bifurcation for the HSS equilibria $B^{\pm}$, PB_4, can be obtained

$$PB_4 : 2ae^4 - e^2k^2 - 2dk^2 = 0. \tag{2.9}$$

The necessary conditions for the Hopf bifurcation points, HB_5 and HB_6, can be obtained

$$HB_5 : 2de^2 - k = 0, HB_6 : e^2k(2ae^4 - 2e^2k^2) - (e^2k^2 - k^2)(2ae^4 + e^4k - e^2k - k^3) = 0 \tag{2.10}$$

Based on the above analyses, we can apply the necessary conditions of the bifurcations to obtain parameter regions corresponding to different number of the equilibria and periodic oscillation. In the following section, we will exhibit complex dynamical behaviors by using XPPAUT packages to verify theoretical results. The system exhibits multiple types of oscillation quenching, i.e., AD and OD, periodic and quasi-periodic oscillations, and their stability coexistence.

3. Numbercial simulations

The dynamics of the coupled VDP system with direct–indirect coupling can be presented by time history and phase diagram for the fixed parameters. To obtain overall perspectives of the dynamical behaviors in system (1.1), we first present bifurcation sets in different parameter spaces to classfiy the number of equilibria and periodic oscillation. Then, one-dimensional bifurcations and corresponding time histories are illustrated to vertify the dynamical classfication by integrating system (1.1) with the fourth-order Runge-Kutta numerical method in Matlab and XPPAUT.

3.1. Dynamics in a-d spaces

In this subsection, we first present the bifurcation sets in the parameter $a - d$ diagram for $e = 1$ and $k = 1$, as shown in Figure 2. It follows that the parameter $a - d$ diagram is divied into $D_1 - D_9$ regions by the pitchfork bifurcation (labeled as PB) curves and the Hopf bifurcation (HB) curves.

In region D_1, system (1.1) proposes a unique trivial equalibrium $O(0, 0, 0, 0, 0)$. With increase of the parameters from D_1 to D_2, the system presents a pair of the IHSS equilibria $A^{\pm}$ by the pitchfork bifurcation of the trivial equalibrium (PB_1), which PB_1 is corresponding to the left equation in Eq (2.2). Further, the pair of the IHSS equilibria $A^{\pm}$ loses its stability by the Hopf bifucation (HB_4) in correspondence with Eq (2.6). The system exhibits a pair of periodic orbit surrounded by the IHSS equilibria $A^{\pm}$ in region D_3. Employing the pitchfork bifurcation of the trivial equalibrium (PB_2) matching up with Eq (2.2), a new pair of HSS equilibria $B^{\pm}$ will be presented in region D_4, where the system exhibits a trivial equilibrium and two pairs of nontrivial equilibria, i.e., IHSS $A^{\pm}$ and HSS $B^{\pm}$. Moreover, when the parameter crosses the ptichfork bifurcation curve PB_4 connecting with Eq (2.8), the pair of HSS equilibria $B^{\pm}$ will bifurcate into two new pairs of nontrivial equilibria, the NPSS $C^{\pm}, D^{\pm}$ equilibria, respectively. The system (1.1) proposes nine equilibria, including the trivial equilibria O, the IHSS $A^{\pm}$, HSS $B^{\pm}$, and the NPSS $C^{\pm}, D^{\pm}$ equilibria, respectively.

To further explore the dynamics of the coupled VDP system (1.1), we exhibit the one-parameter bifurcation diagram for the fixed parameter $d = 1$ (along Line 1 in Figure 2), as shown in Figure 3(a). The corresponding time histories are shown in Figure 3(b) for the fixed parameters $a = 0.2$, 0.6, 0.8, 1.3, and 1.8, respectively. Here, we present the steady state of the solution for long time iterative computations and throw away its transient state. The unstable equilibria are presented in the dotted line. The numerical simulations agree with the theoretical analysis. It should be noticed that system (1.1) presents stability coexistence with a pair of periodic orbits surrounding the IHSS equilibria $A^{\pm}$ in region D_3. Further, the pair of periodic orbits will bifurcate into a symmetric periodic orbit by employing the fold bifurcation of periodic orbit.

Increasing the parameter a along with Line 2, i.e., $d = 0.35$, the corresponding one-parameter bifurcation diagram is shown in Figure 4(a). It follows that the trivial equilibrium $O(0, 0, 0, 0, 0)$ loses its stability by employing the Hopf bifurcation (HB_1) corresponding with Eq (2.3), which bifurcates into a stable periodic oscillation. In Region D_9, the stable periodic oscillation becomes unstable and turns into a stable quasi-periodic oscillation, and then returns to the stable periodic oscillation by the anti-bifurcation of the quasi-periodic oscillation. Further, the trivial equilibrium $O(0, 0, 0, 0, 0)$ bifurcates into a pair of nontrivial HSS $B^{\pm}$ equilibrium by the pitchfork bifurcation (PB_2) in region D_8. A further pitchfork bifurcation (PB_1) of the trivial equilibrium will induce the pair of nontrivial IHSS $A^{\pm}$ equilibrium in region D_7. Moreover, a new pitchfork bifurcation (PB_3) of the nontrivial IHSS

$A^{\pm}$ equilibrium results in two pairs of nontrivial equilibria, i.e., the NPSS $C^{\pm}, D^{\pm}$ equilibria for the parameter region D_6, which is corresponding to Eq (2.5).

More one-parameter bifurcation diagrams are shown in Figures 4(b)–4(d) for the fixed parameter $d = 0.18$, $d = 0.15$, and $d = 0.1$, respectively. It follows that system (1.1) proposes fewer equilibria with decreasing of the parameter d. When the parameter $d = 0.15$, the system presents two pairs of pitchfork bifurcations of the trivial equilibrium, which induces the IHSS equilibria $A^{\pm}$ and HSS equilibria $B^{\pm}$. Further, there is just a pitchfork bifurcation of the trivial equilibrium surrounded by the periodic solution for $d = 0.1$. In addition, system (1.1) proposes a quasi-periodic oscillation in a wide range of the system parameter a, which is obtained by the quasi-periodic bifurcation of the periodic oscillation. The phase diagram and Poincaré map are shown in Figure 5(a),(b) for the fixed parameters $d = 0.35$, $a = 0.8$ with $e = 1$, $k = 1$. The Poincaré section is chosen as $y = 0$. All numerical results including time histories and bifurcation diagrams all agree with theoretical predictions.

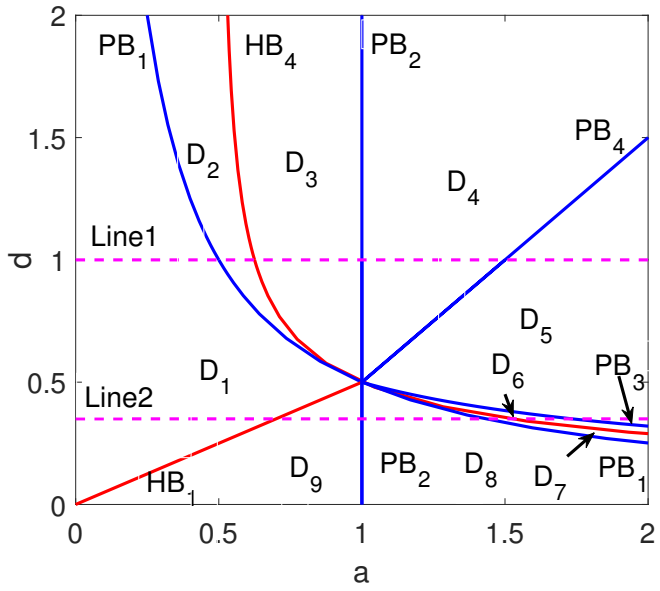

Figure 2. The bifurcation sets in the parameter $a - d$ diagram for $e = 1$ and $k = 1$, where blue solid curve is the pitchfork bifurcation (labeled as PB) and red is for the Hopf bifurcation (HB). The biurcation curves divide the parameter diagram into different regions with different equilibria and periodic oscillation.

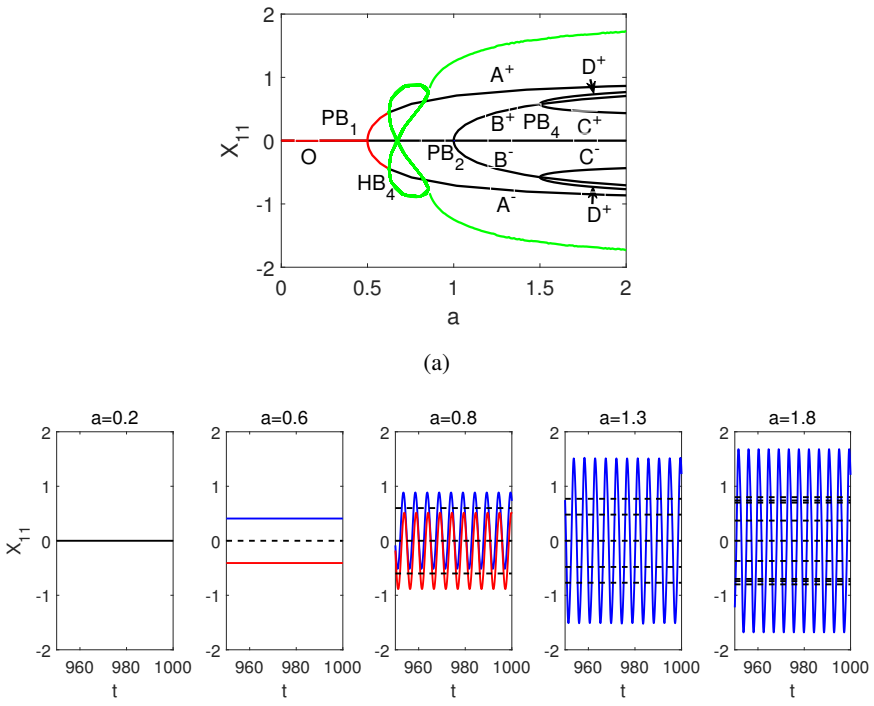

(a)

(b)

Figure 3. (a) The one-parameter bifurcation diagram for $d = 1$ along with Line 1 in Figure 2, where red, black and green solid lines represent stable equilibria, unstable equalibria and stable oscillations, respectively. (b) Time histories for the fixed parameter a, where the dotted line means the unstable equilibria and the solid line means stable equilibria.

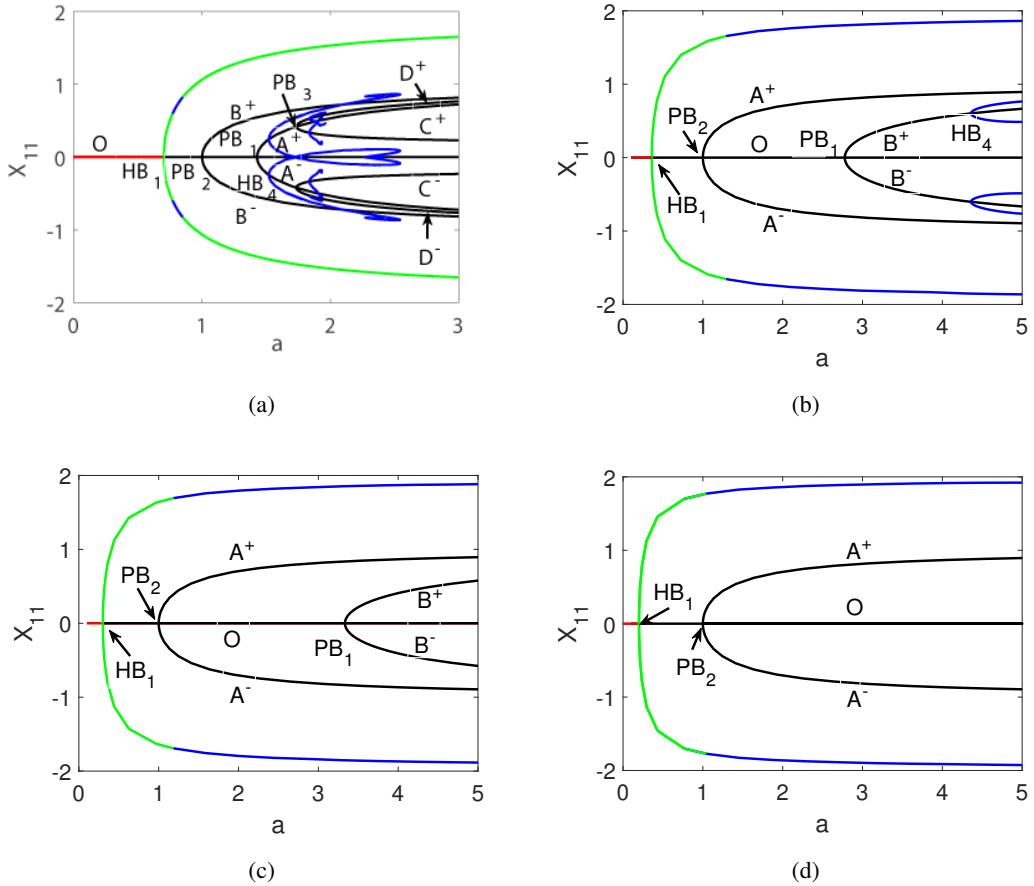

Figure 4. The one-parameter bifurcation diagrams with the increasing parameter a for the fixed d, (a) $d = 0.35$, (b) $d = 0.18$, (c) $d = 0.15$ and (d) $d = 0.1$, respectively. In the diagrams, red, black, blue and green solid lines separately mean stable equalibria, unstable equalibria, unstable oscillations and stable oscillations.

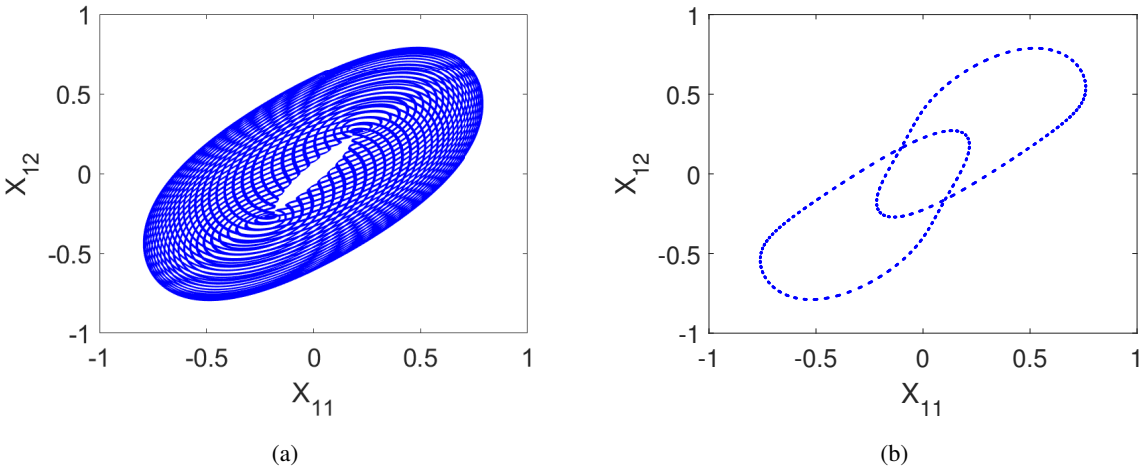

Figure 5. The phase diagram and Poincaré map with $e = 1$, $k = 1$, $d = 0.35$ and $a = 0.8$.

3.2. Dynamics in e-k spaces

Next, we further describe the dynamical behaviors of system (1.1) in the $e - k$ space for the fixed parameters $a = 1$ and $d = 1$. The bifurcation sets are illustrated in Figure 6 by theoretical analysis and numerical simulation.

To more clearly explore the dynamical behavior of system (1.1), we first choose the parameter $k = 1.3$ (Line 1 in Figure 6) and exhibit the one-parameter bifurcation diagram, as shown in Figure 7(a). It follows that system (1.1) proposes the trivial equilibrium and a pair of nontrivial IHSS $A^{\pm}$ equilibria for $e = 0.5$. Further, the system presents a stable periodic oscillation bifurcated from the trivial equilibrium by the subcritical Hopf bifurcation labeled as HB_2, which equals Eq (2.3). In addition, the trivial equilibrium will bifurcate a new pair of the nontrivial HSS $B^{\pm}$ equilibrium by the pitchfork bifurcation PB_2 associated with Eq (2.2). The HSS $B^{\pm}$ will obtain its stability and further bifurcate into two pairs of NPSS equilibria $C^{\pm}, D^{\pm}$ by the PB_4. The two pairs of NPSS equilibria $C^{\pm}, D^{\pm}$ will be eliminated by the subcritical pitchfork bifurcation (PB_3) of the nontrivial IHSS $A^{\pm}$ equilibria, matching with Eq (2.5). The system presents stability coexistence with two pairs of nontrival IHSS $A^{\pm}$ and HSS $B^{\pm}$. Moreover, the system presents a pair of periodic orbits by the anti-Hopf bifurcation of the IHSS $A^{\pm}$ equilibria when the parameter passes through the HB_4 curves. After the parameters pass through HB_4 connecting with Eq (2.6), the system obtains four stable equilibria with two stable equilibria for passing through PB_3. The corresponding time histories are shown in Figure 7(b) for the fixed parameters $e = 0.5$, 1.2, 1.26, 1.3, 2, and 3, respectively.

When we choose $k = 0.95$, i.e., Line 2 in Figure 6, the one-parameter bifurcation diagram is shown in Figure 8(a). It follows that the HSS $B^{\pm}$ equilibria presents a new supercritical anti-Hopf bifurcation curve HB_6. Further, the IHSS $A^{\pm}$ equilibria have the supercritical anti-Hopf bifurcation curve HB_4. Based on these two Hopf bifurctions, system (1.1) illustrates two pairs of stable periodic orbits. The corresponding time history is shown in Figure 9(a), where the parameter is fixed as $e = 1.2$ for $k = 0.95$. In addition, more one-parameter bifurcation diagrams are illustrated in Figures 8(b)–8(d) for the fixed $k = 0.75$, $k = 0.45$, and $k = 0.3$, respectively. It follows that the parameter region of four stable periodic orbits increases with decreasing the parameter k, as shown in Figure 8(b). Meanwhile, we find a region of coexistence between a pair of stable periodic orbits and a pair of stable equilibrium. The time history is shown in Figure 9(b) for $e = 1.5$ with $k = 0.75$. Further, the pair of the large periodic orbit loses its stability by the quasi-periodic bifurcation and translates into a pair of quasi-periodic oscillation, as shown in Figure 8(c). The system (1.1) proposes a pair of stable quasi-periodic oscillation. The parameter region having quasi-periodic oscillation increases with decreasing of the parameter k, as shown in Figure 8(c) for the one-parameter bifurcation diagram with $k = 0.3$. The phase diagram and Poincaré map of the quasi-periodic oscillation are illustrated in Figures 9(c) and 9(d), respectively. It should be noticed that the bifurcation curves, including PB and HB, correspond to different equilibria, i.e., the trivial equilibrium O, and nontrivial equilibria IHSS $A^{\pm}$ and HSS $B^{\pm}$. For the same equilibrium, there are several intersections of different bifurcation curves, such as PB_2-HB_2, PB_3-HB_4, PB_4-HB_6. These intersection points are to the pitchfork–Hopf bifurcation, which is a codimension two bifurcation. The system may present more complex and interesting dynamical behaviors near the bifurcation points.

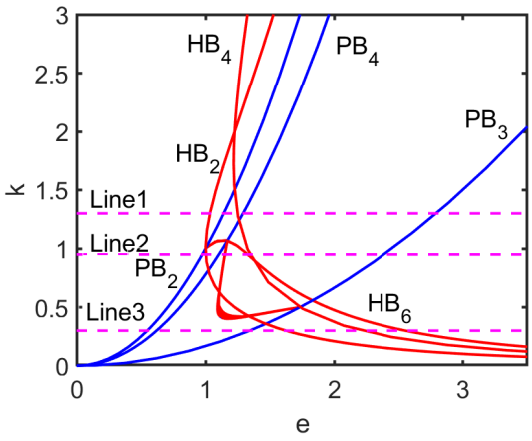

Figure 6. The two-parameter $e-k$ bifurcation diagram with $a = 1$ and $k = 1$. Blue lines mean pitchfork bifurcations labeled as PB and red lines mean Hopf bifurcations labeled as HB.

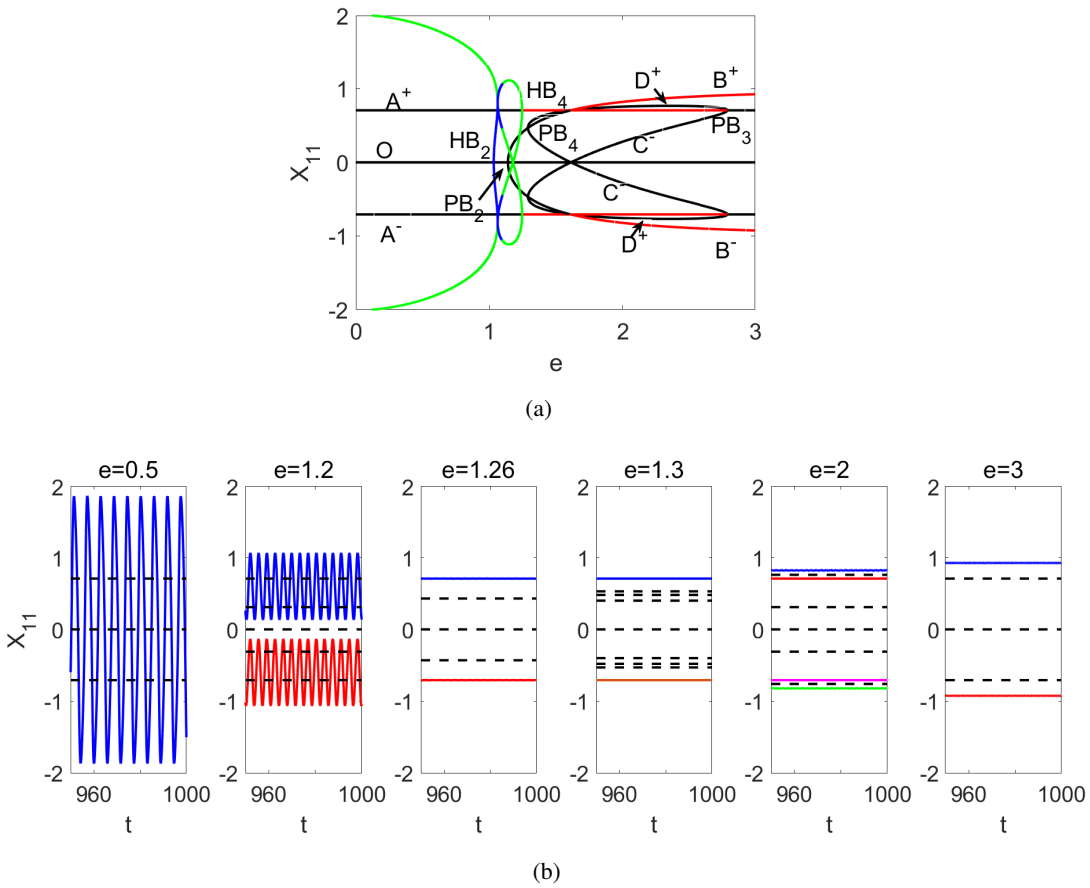

Figure 7. (a) The one-parameter bifurcation diagram for $k = 1.3$ along with Line 1 in Figure 6, where red, black, blue and green solid lines mean stable equilibria, unstable equilibria, unstable oscillations and stable oscillations, respectively. (b) Time histories for the fixed parameter e, where the dotted line means the unstable equilibria.

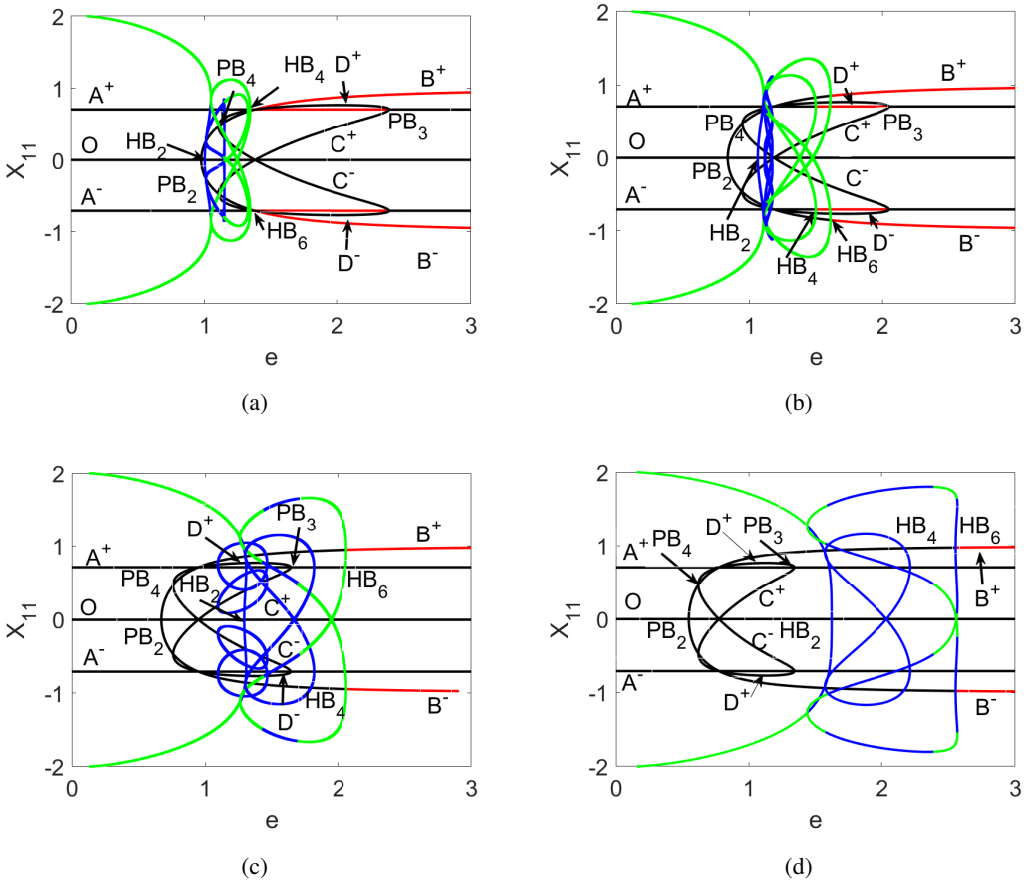

Figure 8. The one-parameter bifurcation diagrams with the increasing parameter e for the fixed parameter k, (a) $k = 0.95$, (b) $k = 0.75$, (c) $k = 0.45$, and (d) $k = 0.3$, respectively, where the red solid line means stable equalibria, the black solid line means unstable equalibria, the blue solid line means unstable oscillations and the green solid line means stable oscillations.

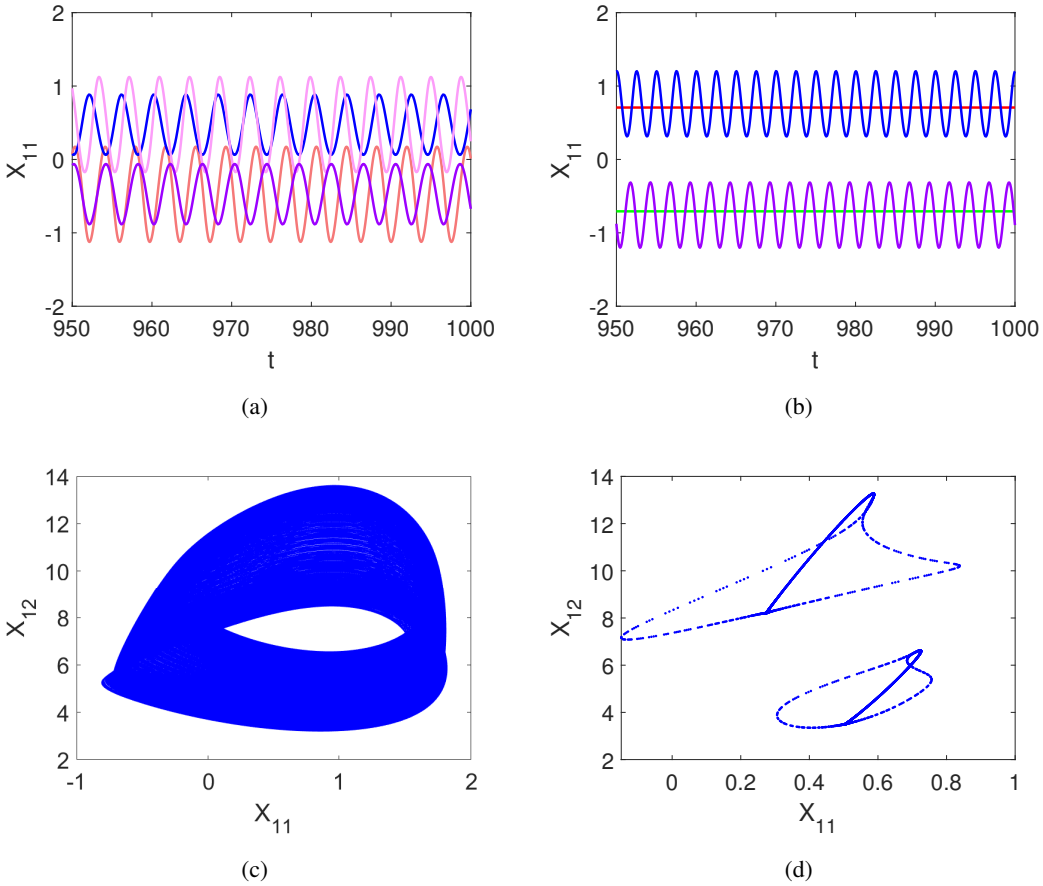

Figure 9. (a) The time history of two pairs of periodic orbits with $e = 1.2$ for $k = 0.95$. (b) The time history of a pair of periodic orbit and a pair of equilibrium with $e = 1.5$ for $k = 0.75$. (c) The phase diagram of the quasi-periodic oscillation with $e = 2$ for $k = 0.3$.(d) The corresponding Poincaré map of the quasi-periodic oscillation.

4. Conclusions and discussion

In this paper, we investigated the stable equilibria and oscillations with homogeneous or inhomogeneous patterns in a pair of VDP oscillators with direct-indirect coupling. The system presented several types of oscillation quenching such as AD, OD and their stable coexistence. In addition, by employing the pitchfork and Hopf bifurcations of the trivial and nontrivial equilibria, we illustrated in detail the dynamical mechanisms of the periodic and quasi-periodic oscillations in the different parameter spaces. The results show that the coupled VDP oscillator presented two pairs of periodic oscillations by the anti-Hopf bifurcation of the IHSS and HSS equilibria. Further, the stability coexistence with a pair of equilibria and a pair of periodic oscillations have been illustrated in some regions of the parameters.

As a matter of fact, in order to demonstrate a steady state and an oscillatory state with homogeneous or inhomogeneous patterns, many types of coupling models have been proposed, such as diffusion coupling [30], mean-field diffusion coupling [31–34], time-delay coupling [35–38], conjugate coupling [39, 40], direct and indirect coupling [9, 24, 41], repulsive coupling [42, 43] and indirect

coupling [44–46]. The system model with direct-indirect coupling was originally proposed by Resmi et al. [24] and showed that it can induce AD. Detailed bifurcation of the coupled nonlinear oscillator with the coupling scheme was illustrated in [9], which induced an OD state and an NAD state. Further, they presented transition scenarios from AD to OD within parameter space by employing experiment researches. In the present paper, we first reported the multiple types of stable coexistence including the coexistence of two oscillations, the coexistence of oscillations and equilibria and the coexistence of multiple equilibria. Meanwhile, we have discussed the dynamic mechanism about generating the phenomena.

The application of this system model is extensive. For example, direct-indirect coupling can help understand the light-feeding phase relations on entraining robust circadian rhythms in the periphery [29], where it is associated with phase-filp behavior. In neural networks, it also can help improve the capacity of efficient reservior computing inspired by the brain [47]. In the realm of biological nervous systems, the coupling scheme is also of great significance, as nerve cells can interact directly through electrical synapses or gap junctions, and indirectly through the shared internal environment. Meanwhile, three types of coexistence mentioned above have been observed in biological networks, such as genetic networks [48] and slime networks [49]. We believe that it can help us understand the dynamic behavior in many biological processes, such as cell-to-cell communication. Future research can be undertaken in order to explore the role of the direct-indirect coupling studied here in inducing the three types of coexistence in biological systems.

Use of AI tools declaration

The authors declare they have not used Artificial Intelligence (AI) tools in the creation of this article.

Acknowledgments

This research is supported by the National Natural Science Foundation of China under Grant Nos. 12172212 and 11932015 and the Fundamental Research Funds for the Central Universities (No. 22120220588).

Conflict of interest

The authors declare that there is no conflict of interest.

References

1. A. Pikovsky, M. Rosenblum, J. Kurths, *Synchronization: A Universal Concept in Nonlinear Sciences*, Cambridge Nonlinear Science Series, Cambridge University Press, 2010. https://doi.org/10.1017/CBO9780511755743
2. K. Kaneko, Theory and applications of coupled map lattices, in *Nonlinear Science: Theory and Applications*, Wiley–Blackwell, 1993. Available from: https://cir.nii.ac.jp/crid/1573105973923422464.

3. E. Ott, K. Wiesenfeld, *Chaos in Dynamical Systems*, *Phys. Today*, **47** (1994). https://doi.org/10.1063/1.2808369
4. G. Saxena, A. Prasad, R. Ramaswamy, Amplitude death: the emergence of stationarity in coupled nonlinear systems, *Phys. Rep.*, **521** (2012), 205–228. https://doi.org/10.1016/j.physrep.2012.09.003
5. P. Kumar, A. Prasad, R. Ghosh, Stable phase-locking of an external-cavity diode laser subjected to external optical injection, *J. Phys. B: At. Mol. Opt. Phys.*, **41** (2008), 135402. https://doi.org/10.1088/0953-4075/41/13/135402
6. B. Gallego, P. Cessi, Decadal variability of two oceans and an atmosphere, *J. Clim.*, **14** (2001), 2815–2832. https://doi.org/10.1175/1520-0442(2001)014<2815:DVOTOA>2.0.CO;2
7. H. Zhang, D. Xu, C. Lu, E. Qi, J. Hu, Y. Wu, Amplitude death of a multi-module floating airport, *Nonlinear Dyn.*,**79** (2015), 2385–2394. https://doi.org/10.1007/s11071-014-1819-x
8. T. Banerjee, D. Biswas, Amplitude death and synchronized states in nonlinear time-delay systems coupled through mean-field diffusion, *Chaos*, **23** (2013), 043101. https://doi.org/10.1063/1.4823599
9. D. Ghosh, T. Banerjee, Transitions among the diverse oscillation quenching states induced by the interplay of direct and indirect coupling, *Phys. Rev. E: Stat. Nonlinear Soft Matter Phys.*, **90** (2014), 062908. https://doi.org/10.1103/PhysRevE.90.062908
10. G. B. Ermentrout, N. Kopell, Oscillator death in systems of coupled neural oscillators, *SIAM J. Appl. Math.*, **50** (1990), 125–146. https://doi.org/10.1137/0150009
11. A. Koseska, E. Volkov, J. Kurths, Oscillation quenching mechanisms: amplitude vs. oscillation death, *Phys. Rep.*, **531** (2013), 173–199. https://doi.org/10.1016/j.physrep.2013.06.001
12. R. Curtu, Singular Hopf bifurcations and mixed-mode oscillations in a two-cell inhibitory neural network, *Physica D*, **239** (2010), 504–514. https://doi.org/10.1016/j.physd.2009.12.010
13. A. Koseska, E. Volkov, J. Kurths, Parameter mismatches and oscillation death in coupled oscillators, *Chaos*, **20** (2010), 023132. https://doi.org/10.1063/1.3456937
14. N. Suzuki, C. Furusawa, K. Kaneko, Oscillatory protein expression dynamics endows stem cells with robust differentiation potential, *PLoS One*, **6** (2011), e27232. https://doi.org/10.1371/journal.pone.0027232
15. D. Biswas, N. Hui, T. Banerjee, Amplitude death in intrinsic time-delayed chaotic oscillators with direct–indirect coupling: the existence of death islands, *Nonlinear Dyn.*, **88** (2017), 2783–2795. https://doi.org/10.1007/s11071-017-3411-7
16. A. H. Nayfeh, D. T. Mook, *Nonlinear Oscillations*, John Wiley & Sons, 2008.
17. A. Anees, Z. Ahmed, A technique for designing substitution box based on van der pol oscillator, *Wireless Pers. Commun.*, **82** (2015), 1497–1503. https://doi.org/10.1007/s11277-015-2295-4
18. G. Juárez, M. Ramírez-Trocherie, Á. Báez, A. Lobato, E. Iglesias-Rodríguez, P. Padilla, et al., Hopf bifurcation for a fractional van der Pol oscillator and applications to aerodynamics: implications in flutter, *J. Eng. Math.*, **139** (2023), 1–15. https://doi.org/10.1007/s10665-023-10258-7
19. S. Dutta, N. R. Cooper, Critical response of a quantum van der Pol oscillator, *Phys. Rev. Lett.*, **123** (2019), 250401. https://doi.org/10.1103/PhysRevLett.123.250401

20. S. Wirkus, R. Rand, The dynamics of two coupled van der Pol oscillators with delay coupling, *Nonlinear Dyn.*, **30** (2002), 205–221. https://doi.org/10.1023/A:1020536525009

21. E. Camacho, R. Rand, H. Howland, Dynamics of two van der Pol oscillators coupled via a bath, *Int. J. Solids Struct.*, **41** (2004), 2133–2143. https://doi.org/10.1016/j.ijsolstr.2003.11.035

22. K. Konishi, Experimental evidence for amplitude death induced by dynamic coupling: van der Pol oscillators, in *2004 IEEE International Symposium on Circuits and Systems (ISCAS)*, **4** (2004), 792–795. https://doi.org/10.1109/ISCAS.2004.1329123

23. T. Endo, S. Mori, Mode analysis of a ring of a large number of mutually coupled van der Pol oscillators, *IEEE Trans. Circuits Syst.*, **25** (1978), 7–18. https://doi.org/10.1109/TCS.1978.1084380

24. V. Resmi, G. Ambika, R. E. Amritkar, General mechanism for amplitude death in coupled systems, *Phys. Rev. E: Stat. Nonlinear Soft Matter Phys.*, **84** (2011), 046212. https://doi.org/10.1103/PhysRevE.84.046212

25. D. Ghosh, T. Banerjee Mixed-mode oscillation suppression states in coupled oscillators, *Phys. Rev. E: Stat. Nonlinear Soft Matter Phys.*, **92** (2015), 052913. https://doi.org/10.1103/PhysRevE.92.052913

26. C. O. Weiss, R. Vilaseca, Dynamics of lasers, *NASA STI/Recon Tech. Rep. A*, **92** (1991), 39875. Available from: https://ui.adsabs.harvard.edu/abs/1991STIA...9239875W/abstract.

27. K. A. Robbins, A new approach to subcritical instability and turbulent transitions in a simple dynamo, in *Mathematical Proceedings of the Cambridge Philosophical Society*, Cambridge University Press, **82** (1997), 309–325. https://doi/org/10.1017/S0305004100053950

28. B. Ermentrout, *XPPAUT 5.0-the Differential Equations Tool*, University of Pittsburgh, Pittsburgh, 2001.

29. E. X. DeJesus, C. Kaufman, Routh-Hurwitz criterion in the examination of eigenvalues of a system of nonlinear ordinary differential equations, *Phys. Rev. A: At. Mol. Opt. Phys.*, **35** (1987), 5288. https://doi.org/10.1103/PhysRevA.35.5288

30. G. Saxena, A. Prasad, R. Ramaswamy, Amplitude death: the emergence of stationarity in coupled nonlinear systems, *Phys. Rep.*, **521** (2012), 205–228. https://doi.org/10.1016/j.physrep.2012.09.003

31. A. Sharma, M. D. Shrimali Amplitude death with mean-field diffusion, *Phys. Rev. E: Stat. Nonlinear Soft Matter Phys.*, **85** (2012), 057204. https://doi.org/10.1103/PhysRevE.85.057204

32. A. Sharma, K. Suresh, K. Thamilmaran, A. Prasad, M. D. Shrimali, Effect of parameter mismatch and time delay interaction on density-induced amplitude death in coupled nonlinear oscillators, *Nonlinear Dyn.*, **76** (2014), 1797–1806. https://doi.org/10.1007/s11071-014-1247-y

33. T. Banerjee, D. Ghosh, Experimental observation of a transition from amplitude to oscillation death in coupled oscillators, *Phys. Rev. E: Stat. Nonlinear Soft Matter Phys.*, **89** (2014), 062902. https://doi.org/10.1103/PhysRevE.89.062902

34. N. K. Kamal, P. R. Sharma, M. D. Shrimali, Suppression of oscillations in mean-field diffusion, *Pramana*, **84** (2015), 237–247. https://doi.org/10.1007/s12043-015-0929-4

35. A. Zakharova, I. Schneider, Y. N. Kyrychko, K. B. Blyuss, A. Koseska, B. Fiedler, et al., Time delay control of symmetry-breaking primary and secondary oscillation death, *Europhys. Lett.*, **104** (2013), 50004. https://doi.org/10.1209/0295-5075/104/50004

36. D. V. R. Reddy, A. Sen, G. L. Johnston, Time delay induced death in coupled limit cycle oscillators, *Phys. Rev. Lett.*, **80** (1998), 5019. https://doi.org/10.1103/PhysRevLett.80.5109

37. D. V. R. Reddy, A. Sen, G. L. Johnston, Experimental evidence of time-delay-induced death in coupled limit-cycle oscillators, *Phys. Rev. Lett.*, **85** (2000), 3381. https://doi.org/10.1103/PhysRevLett.85.3381

38. F. M. Atay, Distributed delays facilitate amplitude death of coupled oscillators, *Phys. Rev. Lett.*, **91** (2003), 094101. https://doi.org/10.1103/PhysRevLett.91.094101

39. W. Zou, D. V. Senthilkumar, A. Koseska, J. Kurths, Generalizing the transition from amplitude to oscillation death in coupled oscillators, *Phys. Rev. E: Stat. Nonlinear Soft Matter Phys.*, **88** (2013), 050901. https://doi.org/10.1103 /PhysRevE.88.050901

40. R. Karnatak, R. Ramaswamy, A. Prasad, Amplitude death in the absence of time delays in identical coupled oscillators, *Phys. Rev. E: Stat. Nonlinear Soft Matter Phys.*, **76** (2007), 035201. https://doi.org/10.1103/PhysRevE.76.035201

41. A. Sharma, P. R. Sharma, M. D. Shrimali, Amplitude death in nonlinear oscillators with indirect coupling, *Phys. Lett. A*, **376** (2012), 1562–1566. https://doi.org/10.1016/j.physleta.2012.03.033

42. C. R. Hens, O. I. Olusola, P. Pal, S. K. Dana, Oscillation death in diffusively coupled oscillators by local repulsive link, *Phys. Rev. E: Stat. Nonlinear Soft Matter Phys.*, **88** (2013), 034902. https://doi.org/10.1103/PhysRevE.88.034902

43. B. K. Bera, C. Hens, D. Ghosh, Emergence of amplitude death scenario in a network of oscillators under repulsive delay interaction, *Phys. Lett. A*, **380** (2016), 2366–2373. https://doi.org/10.1016/j.physleta.2016.05.028

44. N. K. Kamal, P. R. Sharma, M. D. Shrimali, Oscillation suppression in indirectly coupled limit cycle oscillators, *Phys. Rev. E: Stat. Nonlinear Soft Matter Phys.*, **92** (2015), 022928. https://doi.org/10.1103/PhysRevE.92.022928

45. P. R. Sharma, N. K. Kamal, U. K. Verma, K. Suresh, K. Thamilmaran, M. D. Shrimali, Suppression and revival of oscillation in indirectly coupled limit cycle oscillators, *Phys. Lett. A*, **380** (2016), 3178–3184. https://doi.org/10.1016/j.physleta.2016.07.041

46. A. Sharma, U. K. Verma, M. D. Shrimali, Phase-flip and oscillation-quenching-state transitions through environmental diffusive coupling, *Phys. Rev. E: Stat. Nonlinear Soft Matter Phys.*, **94** (2016), 062218. https://doi.org/10.1103/PhysRevE.94.062218

47. J. Choi, P. Kim, Reservoir computing based on quenched chaos, *Chaos, Solitons Fractals*, **140** (2020), 110131. https://doi.org/10.1016/j.chaos.2020.110131

48. E. Ullner, A. Zaikin, E. I. Volkov, J. García-Ojalvo, Multistability and clustering in a population of synthetic genetic oscillators via phase-repulsive cell-to-cell communication, *Phys. Rev. Lett.*, **99** (2007), 148103. https://doi.org/10.1103/PhysRevLett.99.148103

49. A. Takamatsu, Spontaneous switching among multiple spatio-temporal patterns in three-oscillator systems constructed with oscillatory cells of true slime mold, *Physica D*, **223** (2006), 180–188. https://doi.org/10.1016/j.physd.2006.09.001

AIMS Press